Acta Cryst E CRYSTALLOGRAPHIC COMMUNICATIONS

ISSN 2056-9890

Synthesis and structure of *trans*-2,5-dimethylpiperazine-1,4-diium dihydrogen diphosphate

Houda Mrad,[a]* Adel Elboulali,[a] Benoît Baptiste[b] and Samah Akriche[a]

[a]Laboratory of Materials Chemistry (LR13ES08), Faculty of Sciences of Bizerte, University of Carthage, 7021 Zarzouna, Bizerte, Tunisia, and [b]Institut de Minéralogie, de Physique des Matériaux et de, Cosmochimie CNRS - UMR 7590, Plateforme de diffraction des rayons X, 75005 Paris, France. *Correspondence e-mail: houda.mrad@fsb.ucar.tn

Received 10 October 2024
Accepted 17 October 2024

Edited by W. T. A. Harrison, University of Aberdeen, United Kingdom

Keywords: crystal structure; Hirshfeld surface analysis; dihydrogen diphosphate; *trans*-2,5-dimethylpiperazine.

CCDC reference: 2386600

Supporting information: this article has supporting information at journals.iucr.org/e

In the title salt, $C_6H_{16}N_2^{2+}\cdot H_2P_2O_7^{2-}$, the complete dication is generated by a crystallographic centre of symmetry with the methyl groups in equatorial orientations. The complete dianion is generated by a crystallographic twofold axis with the central O atom lying on the axis: the P—O—P bond angle is 135.50 (12)°. In the crystal, the dihydrogen diphosphate anions are linked by O—H···O hydrogen bonds, generating (001) layers. The organic cations bond to the inorganic layers by way of N—H···O and C—H···O hydrogen bonds. A Hirshfeld surface analysis shows that the most important contributions for the crystal packing are from O···H/H···O (60.5%) and H···H (39.4%) contacts.

1. Chemical context

Hybrid organic–diphosphate-based materials have received attention due to their role in catalytic, adsorption, ion-exchange, optical and biological processes (Chen & Munson, 2002; Ballarini *et al.*, 2006). Protonated diphosphate forms such as $HP_2O_7^{3-}$ or $H_2P_2O_7^{2-}$ have the ability to associate with organic cations by means of ionic and non-covalent interactions (Desiraju, 1989; Steiner, 2002) to generate different supramolecular architectures. Among the many diphosphate structures templated with organic cations are $(C_2H_{10}N_2)\cdot H_2P_2O_7$ (Averbuch-Pouchot & Durif, 1993), $(C_5H_6N_2O_2)_2\cdot H_2P_2O_7$ (Toumi Akriche *et al.*, 2010), $(C_8H_{12}N)_2\cdot H_2P_2O_7$, (Marouani *et al.*, 2010 $(C_8H_{12}NO)_2\cdot H_2P_2O_7$ (Elboulali *et al.*, 2013) and $(C_6H_5CH_2NH_3)_2\cdot H_2P_2O_7$ (Saad *et al.*, 2014). As part of our ongoing studies of these compounds, we now report the synthesis and structure of the title compound, $C_6H_{16}N_2^{2+}\cdot H_2P_2O_7^{2-}$, (I).

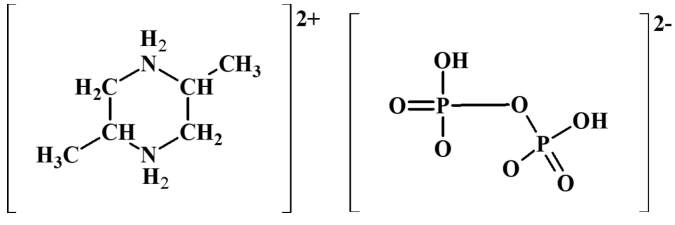

2. Structural commentary

The asymmetric unit of (I) comprises a half diphosphate anion completed by a crystallographic twofold rotation axis (atom O4 lies on the axis) and half a *trans*-2,5-dimethylpiperazine-1,4-dium cation completed by inversion symmetry (Fig. 1). The phosphorous atom adopts a distorted tetrahedral geometry with bond lengths and angles in the range 1.4916 (11)–1.5884 (8) Å and 102.44 (9)–116.60 (8)°, respectively. The

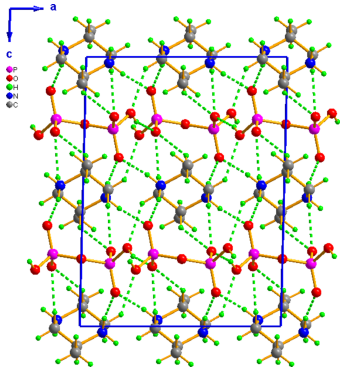

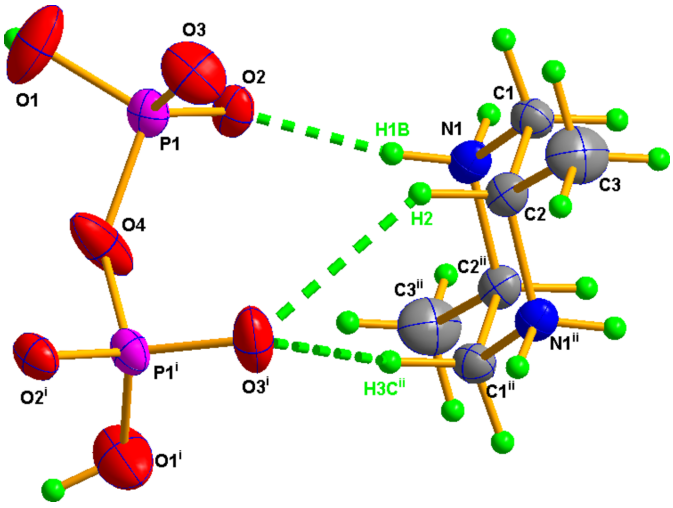

Figure 1
The molecular structure of (I) with displacement ellipsoids drawn at the 50% probability level. Symmetry codes: (i) $-x+1, y, -z+\frac{1}{2}$; (ii) $-x+1, -y+1, -z+1$. The H atoms are presented as small spheres of arbitrary radius. Hydrogen bonds are shown as green dotted lines.

longest P—O distance corresponds to the bridging oxygen atom [P1—O4 = 1.5884 (8) Å], the intermediate one is the P—OH bond [P1—O1 = 1.5389 (15) Å], whereas the shortest bonds correspond to terminal oxygen atoms [P1—O2 = 1.4916 (11) and P1—O3 = 1.4924 (14) Å] in agreement with previous dihydrogen diphosphate structures elaborated by our group (Toumi Akriche *et al.*, 2010; Saad *et al.*, 2014). The PO_4 tetrahedra are fused by atom O4 forming a bent P_2O_7 unit [P1—O4—P1^{i} = 135.50 (12)°; symmetry code: (i) $-x+1, y, -z+\frac{1}{2}$)] and staggered conformation [O1—P1—P1^{i}—O2^{i} = 42.8 (1)°], close to those previously observed for diphosphates with twofold symmetry (Marouani *et al.*, 2010; Charfi & Jouini, 1997). In the cation, the piperazine ring adopts a chair conformation with puckering parameters Q = 0.2770 Å, θ = 90° and φ = 142° in which the methyl substituents occupy equatorial sites. The bonds and angles in the cation [N/C—C in the range 1.484 (2)–1.514 (2) Å and N/C—C/N—C, in the range 108.68 (11)–112.80 (12)°] show no significant difference from those reported in other *trans*-2,5-dimethylpiperazine based salts (Landolsi & Abid, 2021; Gatfaoui *et al.*, 2014).

Table 1
Hydrogen-bond geometry (Å, °).

D—H···A	D—H	H···A	D···A	D—H···A
O1—H1···O3^{i}	0.88 (3)	1.61 (3)	2.460 (2)	161 (3)
N1—H1A···O2^{ii}	0.90 (2)	1.86 (2)	2.7454 (17)	167 (2)
N1—H1B···O2	0.90 (2)	1.87 (2)	2.7543 (17)	168 (2)
C1—H1C···O3^{iii}	0.982 (19)	2.353 (19)	3.193 (2)	143.0 (15)
C1—H1D···O1^{iv}	0.970 (19)	2.41 (2)	3.205 (2)	139.1 (15)
C2—H2···O3^{v}	1.00 (2)	2.53 (2)	3.344 (2)	138.3 (15)

Symmetry codes: (i) $-x+\frac{3}{2}, y-\frac{1}{2}, -z+\frac{1}{2}$; (ii) $-x+\frac{3}{2}, -y+\frac{1}{2}, -z+1$; (iii) $x, -y+1, z+\frac{1}{2}$; (iv) $-x+\frac{3}{2}, y+\frac{1}{2}, -z+\frac{1}{2}$; (v) $-x+1, y, -z+\frac{1}{2}$.

3. Supramolecular features

The extended structure of (I) is built up from hydrogen-bonded sheets of diphosphate anions extended along the crystallographic c-axis direction at z = 1/4 and 3/4 with the cations lying between these anionic sheets featuring extensive hydrogen bonds, so as to build a three-dimensional supramolecular network (Fig. 2). A projection along the c axis at z = 1/4 of the inorganic sheet (Fig. 3) shows that O—H···O hydrogen bonds (Table 1) link adjacent dihydrogen diphos-

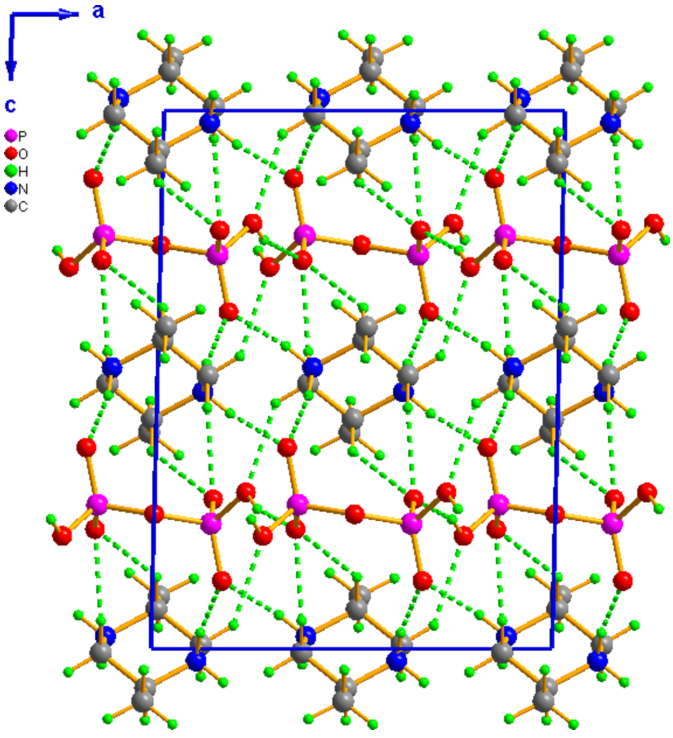

Figure 2
The projection along the b-axis direction of the crystal packing of (I). Hydrogen bonds are shown as dotted lines.

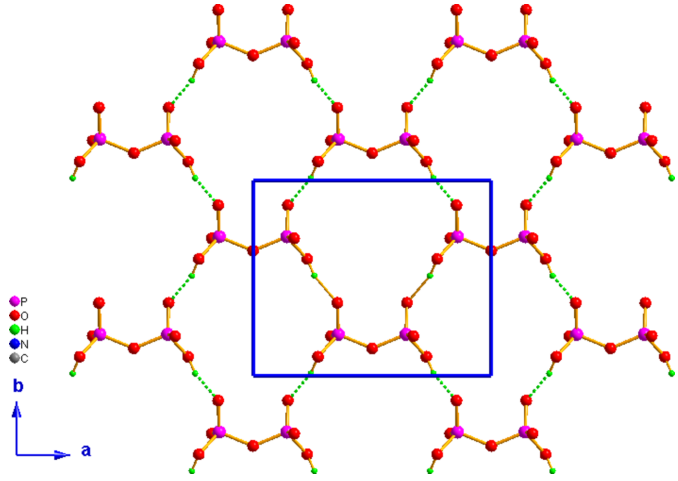

Figure 3
The layered dihydrogen diphosphate self-assembly, viewed along the c axis at z = 1/4. The O—H···O hydrogen bonds are shown as green dotted lines.

phate anions to develop anionic layers extending parallel to (001). Electrostatic, medium-strength N—H···O and weaker C—H···O interactions (Table 1) between the organic cations and these anionic layers are responsible for the three-dimensional crystal structure.

4. Hirshfeld surface analysis

Fig. 4*a* shows the Hirshfeld surface generated with Crystal Explorer (Wolff *et al.*, 2012) mapped over d_{norm} with red spots corresponding to short inter-atomic contacts. The fingerprint plots illustrated in Fig. 4*b* and 4*c* with characteristic spikes indicate that the major inter-atomic contributions to the structure are from O···H/H···O (60.5%) and H···H (39.4%) contacts in accordance with the structure topology.

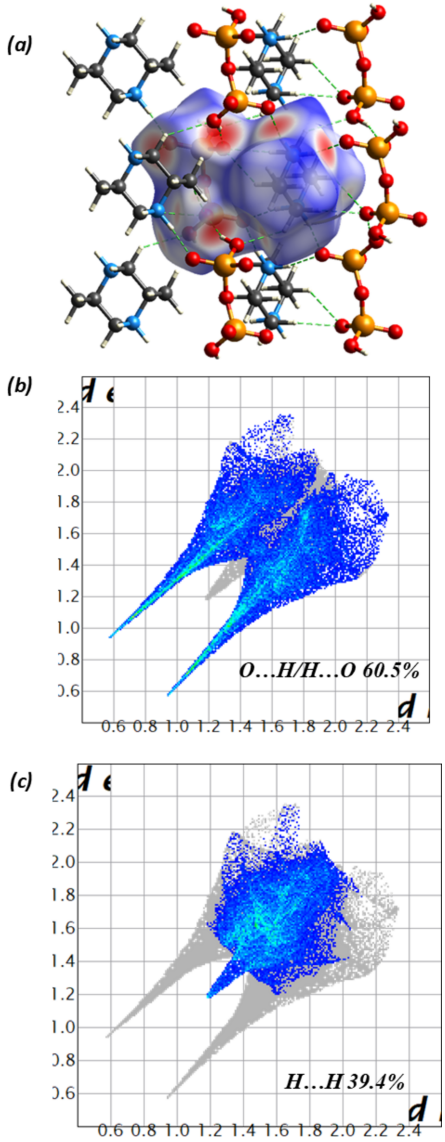

Figure 4
Hirshfeld surface (*a*) mapped with d_{norm} and fingerprint plots showing the major inter-contacts contributions of (*b*) O···H/H···O and (*c*) H···H.

5. Synthesis and experimental

The monocrystals of (I) were synthesized into two steps. Firstly, diphosphoric acid, $H_4P_2O_7$, was obtained from $Na_4P_2O_7$ (26 mg, 50 ml H_2O) by using an ion-exchange resin (Amberlite IR 120). Then, the fresh diphosphoric acid solution was neutralized with *trans*-2,5-dimethylpiperazine base in a 1:1 molar ratio at low temperature. The resulting solution was slowly evaporated at room temperature for several days until colourless needle-shaped crystals of (I) were grown.

6. IR spectrum

The IR spectrum of (I) was collected at room temperature using a Perkin–Elmer Spectrum BXII spectrometer (KBr method) between 400 and 4000 cm^{-1} (Fig. 5). The spectrum exhibits broad bands between 2376 and 3027 cm^{-1}, which can be assigned to the stretching modes of the $–CH_3$, $–CH_2–$, –CH– and $(–NH_2)^+$ groups of the organic cation (Silverstein *et al.*, 1974). The broadness of these bands in (I) is indicative of the presence of a hydrogen-bonding network. The bending vibrations of these groups are observed in the region 1321–1631 cm^{-1}. The internal modes of the $(H_2P_2O_7)^{2-}$ anion appear in the range 410–1265 cm^{-1} (Harcharras *et al.*, 1997; Kamoun *et al.*, 1992). The elongation modes of the PO_2 and PO_3 terminal groups occur between 1265 and 975 cm^{-1}, whereas the terminal P—O stretching vibration of the PO_2 group is observed at 1155 cm^{-1} and those at 1093 and 1051 cm^{-1} are attributed to the symmetric and asymmetric terminal P—O stretching vibration of the PO_3 group (Sarr & Diop, 1987). The rocking of the PO_2 and PO_3 deformation modes occur between 491 and 627 cm^{-1}. The symmetric and asymmetric elongation modes of the P—O—P bridge for the diphosphate group with a bent conformation are observed as ν_{as}(P—O—P) = 911 and 975 cm^{-1} and ν_s(P—O—P)=

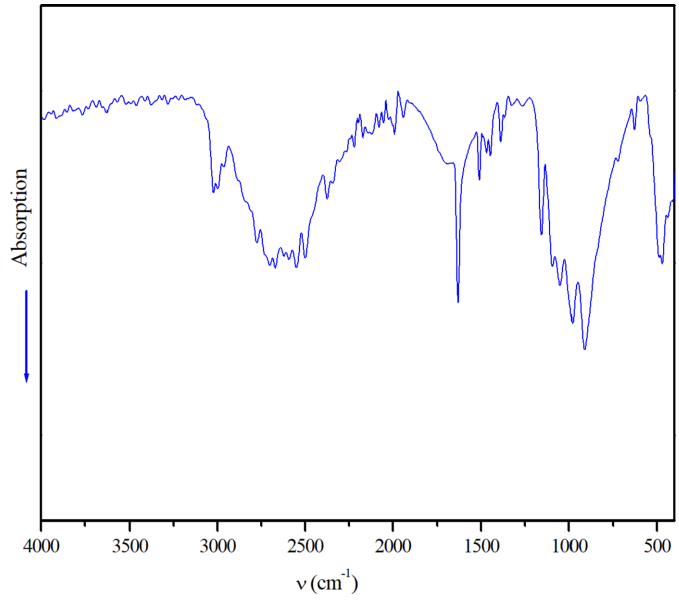

Figure 5
The infrared spectrum of (I).

721 cm^{-1}. The simultaneous activity of these vibration modes confirms the results obtained by X-ray concerning the bent geometry and the C_2 symmetry of the diphosphate anion. With regard to the Lazarev (1972) correlation between the P—O—P bridge stretching frequencies and the bridge angle value as $\Delta = (\nu_{as} - \nu_s)/(\nu_{as} + \nu_s) = 0.12$, and by simple extrapolation of the graph of $\Delta = f(\alpha)$ given by Rulmont *et al.* (1991), we can estimate the calculated P—O—P angle of 136° in excellent agreement with the value of 135.50 (12)° found for (I).

7. Refinement

Crystal data, data collection and structure refinement details are summarized in Table 2. All H atoms were located in a difference Fourier map and their positions were freely refined.

Table 2
Experimental details.

Crystal data	
Chemical formula	$C_6H_{16}N_2^{2+}\cdot H_2O_7P_2^{2-}$
M_r	292.16
Crystal system, space group	Monoclinic, *C*2/*c*
Temperature (K)	293
a, *b*, *c* (Å)	10.2557 (5), 8.3978 (5), 13.7681 (7)
β (°)	91.422 (4)
V (Å^3)	1185.42 (11)
Z	4
Radiation type	Mo *K*α
μ (mm^{-1})	0.39
Crystal size (mm)	0.30 × 0.20 × 0.10
Data collection	
Diffractometer	Xcalibur diffractometer with Sapphire3 CCD detector
Absorption correction	Multi-scan (*CrysAlis PRO*; Rigaku OD, 2019)
T_{min}, T_{max}	0.979, 1.000
No. of measured, independent and observed [$I > 2\sigma(I)$] reflections	9376, 2255, 1738
R_{int}	0.040
(sin $\theta/\lambda)_{max}$ (Å^{-1})	0.769
Refinement	
$R[F^2 > 2\sigma(F^2)]$, $wR(F^2)$, *S*	0.041, 0.103, 1.05
No. of reflections	2255
No. of parameters	114
H-atom treatment	All H-atom parameters refined
$\Delta\rho_{max}$, $\Delta\rho_{min}$ (e Å^{-3})	0.59, −0.39

Computer programs: *CrysAlis PRO* (Rigaku OD, 2019), *SHELXS97* (Sheldrick, 2008), *SHELXL2018/3* (Sheldrick, 2015), *DIAMOND* (Brandenburg & Putz, 2005) and *WinGX* publication routines (Farrugia, 2012).

Acknowledgements

We thank Professor Baptiste Benoît from the IMPMC of the Sorbonne University for collecting the intensity data.

Funding information

This work was supported by the Tunisian Ministry of Higher Education Scientific Research.

References

Averbuch-Pouchot, M. T. & Durif, A. (1993). *C. R. Acad. Sci.* **316**, 187–192.

Ballarini, N., Cavani, F., Cortelli, C., Ligi, S., Pierelli, F., Trifirò, F., Fumagalli, C., Mazzoni, G. & Monti, T. (2006). *Top. Catal.* **38**, 147–156.

Brandenburg, K. & Putz, H. (2005). *DIAMOND*. Crystal Impact GbR, Bonn, Germany.

Charfi, M. & Jouini, A. (1997). *Acta Cryst.* C**53**, 463–465.

Chen, B. & Munson, E. J. (2002). *J. Am. Chem. Soc.* **124**, 1638–1652.

Desiraju, G. R. (1989). In *Crystal Engineering: The Design of Organic Solids*. Amsterdam: Elsevier.

Elboulali, A., Akriche, S., Al-Deyab, S. S. & Rzaigui, M. (2013). *Acta Cryst.* E**69**, o213–o214.

Farrugia, L. J. (2012). *J. Appl. Cryst.* **45**, 849–854.

Gatfaoui, S., Roisnel, T., Dhaouadi, H. & Marouani, H. (2014). *Acta Cryst.* E**70**, o725.

Harcharras, M., Ennaciri, A., Rulmont, A. & Gilbert, B. (1997). *Spectrochim. Acta A Mol. Biomol. Spectrosc.* **53**, 345–352.

Kamoun, S., Jouini, A. & Daoud, A. (1992). *J. Solid State Chem.* **99**, 18–28.

Landolsi, M. & Abid, S. (2021). *Acta Cryst.* E**77**, 424–427.

Lazarev, A. N. (1972). *Vibrational spectra and structure of silicates*, translated by G. D. Archard. New York and London: Consultants Bureau.

Marouani, H., Elmi, L., Rzaigui, M. & Al-Deyab, S. S. (2010). *Acta Cryst.* E**66**, o535.

Rigaku OD (2019). *CrysAlis PRO*. Oxford Diffraction Ltd, Yarnton, England.

Rulmont, A., Cahay, A., Liegeois-Duyckerts, R. & Tarte, M. (1991). *Eur. J. Solid State Inorg. Chem.* **28**, 207–000.

Saad, A. B., Elboulali, A., Ratel-Ramond, N., Mohamed, R. & Toumi, S. A. (2014). *Acta Cryst.* E**70**, o3.

Sarr, O. & Diop, L. (1987). *Spectrochim. Acta A*, **43**, 999–1005.

Sheldrick, G. M. (2008). *Acta Cryst.* A**64**, 112–122.

Sheldrick, G. M. (2015). *Acta Cryst.* C**71**, 3–8.

Silverstein, R. M., Bassler, G. C. & Morrill, T. C. (1974). *Spectrometric identification of organic compounds*, 3rd ed. New York: Wiley.

Steiner, T. (2002). *Angew. Chem. Int. Ed.* **41**, 48–76.

Toumi Akriche, S., Rzaigui, M., Elothman, Z. A. & Mahfouz, R. M. (2010). *Acta Cryst.* E**66**, o358.

Wolff, S. K., Grimwood, D. J., McKinnon, J. J., Turner, M. J., Jayatilaka, D. & Spackman, M. A. (2012). *CrystalExplorer*. University of Western Australia.

supporting information

Acta Cryst. (2024). E**80**, 1202-1205 [https://doi.org/10.1107/S2056989024010132]

Synthesis and structure of *trans*-2,5-dimethylpiperazine-1,4-diium dihydrogen diphosphate

Houda Mrad, Adel Elboulali, Benoît Baptiste and Samah Akriche

Computing details

trans-2,5-Dimethylpiperazine-1,4-diium dihydrogen diphosphate

Crystal data

$C_6H_{16}N_2^{2+}\cdot H_2O_7P_2^{2-}$
M_r = 292.16
Monoclinic, $C2/c$
a = 10.2557 (5) Å
b = 8.3978 (5) Å
c = 13.7681 (7) Å
β = 91.422 (4)°
V = 1185.42 (11) Å^3
Z = 4
$F(000)$ = 616
D_x = 1.637 Mg m^{-3}
Mo $K\alpha$ radiation, λ = 0.71073 Å
Cell parameters from 2302 reflections
θ = 4.0–31.8°
μ = 0.39 mm^{-1}
T = 293 K
Needle, colorless
0.30 × 0.20 × 0.10 mm

Data collection

Xcalibur
diffractometer with Sapphire3 CCD detector
Radiation source: fine-focus sealed X-ray tube, Enhance (Mo) X-ray Source
Graphite monochromator
Detector resolution: 16.0318 pixels mm^{-1}
ω scans
Absorption correction: multi-scan (CrysAlisPro; Rigaku OD, 2019)
T_{min} = 0.979, T_{max} = 1.000
9376 measured reflections
2255 independent reflections
1738 reflections with $I > 2\sigma(I)$
R_{int} = 0.040
θ_{max} = 33.1°, θ_{min} = 3.5°
h = −15→15
k = −12→12
l = −21→21

Refinement

Refinement on F^2
Least-squares matrix: full
$R[F^2 > 2\sigma(F^2)]$ = 0.041
$wR(F^2)$ = 0.103
S = 1.05
2255 reflections
114 parameters
0 restraints
Primary atom site location: structure-invariant direct methods
Secondary atom site location: difference Fourier map
Hydrogen site location: inferred from neighbouring sites
All H-atom parameters refined
$w = 1/[\sigma^2(F_o^2) + (0.038P)^2 + 1.0885P]$ where $P = (F_o^2 + 2F_c^2)/3$
$(\Delta/\sigma)_{max}$ = 0.001
$\Delta\rho_{max}$ = 0.59 e Å^{-3}
$\Delta\rho_{min}$ = −0.38 e Å^{-3}

Special details

Geometry. All esds (except the esd in the dihedral angle between two l.s. planes) are estimated using the full covariance matrix. The cell esds are taken into account individually in the estimation of esds in distances, angles and torsion angles; correlations between esds in cell parameters are only used when they are defined by crystal symmetry. An approximate (isotropic) treatment of cell esds is used for estimating esds involving l.s. planes.

Fractional atomic coordinates and isotropic or equivalent isotropic displacement parameters (Å²)

	x	*y*	*z*	U_{iso}*/U_{eq}
P1	0.64197 (4)	0.21184 (5)	0.26767 (3)	0.02554 (12)
O1	0.72741 (18)	0.0974 (2)	0.20950 (10)	0.0587 (5)
O2	0.67285 (11)	0.20328 (14)	0.37398 (7)	0.0287 (2)
O3	0.64629 (15)	0.37300 (17)	0.22218 (10)	0.0449 (3)
O4	0.5000	0.1402 (2)	0.2500	0.0500 (6)
H1	0.757 (3)	0.012 (4)	0.240 (2)	0.084 (10)*
N1	0.61378 (12)	0.40835 (16)	0.52268 (9)	0.0238 (3)
C1	0.62451 (15)	0.57743 (19)	0.49245 (11)	0.0248 (3)
C2	0.51107 (15)	0.62671 (18)	0.42671 (10)	0.0239 (3)
C3	0.5174 (2)	0.8018 (2)	0.40212 (19)	0.0443 (5)
H1A	0.683 (2)	0.385 (3)	0.5625 (16)	0.042 (6)*
H1B	0.622 (2)	0.345 (3)	0.4707 (16)	0.039 (6)*
H1C	0.6259 (18)	0.642 (2)	0.5518 (14)	0.028 (5)*
H1D	0.7042 (19)	0.588 (2)	0.4565 (14)	0.032 (5)*
H2	0.510 (2)	0.559 (3)	0.3668 (15)	0.039 (5)*
H3A	0.516 (3)	0.862 (4)	0.460 (2)	0.084 (10)*
H3B	0.442 (3)	0.833 (3)	0.359 (2)	0.064 (8)*
H3C	0.603 (3)	0.817 (3)	0.3694 (19)	0.061 (7)*

Atomic displacement parameters (Å²)

	U^{11}	U^{22}	U^{33}	U^{12}	U^{13}	U^{23}
P1	0.0296 (2)	0.0287 (2)	0.01809 (17)	0.00277 (15)	−0.00450 (13)	0.00137 (14)
O1	0.0792 (12)	0.0686 (11)	0.0291 (7)	0.0334 (9)	0.0148 (7)	−0.0004 (7)
O2	0.0323 (6)	0.0344 (6)	0.0189 (5)	0.0073 (5)	−0.0055 (4)	−0.0012 (4)
O3	0.0556 (9)	0.0387 (7)	0.0400 (7)	−0.0063 (6)	−0.0100 (6)	0.0169 (6)
O4	0.0415 (11)	0.0244 (9)	0.0823 (15)	0.000	−0.0347 (10)	0.000
N1	0.0225 (6)	0.0279 (6)	0.0210 (5)	0.0053 (5)	−0.0025 (4)	0.0010 (5)
C1	0.0233 (6)	0.0276 (7)	0.0233 (6)	−0.0022 (5)	−0.0009 (5)	0.0008 (5)
C2	0.0252 (7)	0.0260 (7)	0.0206 (6)	0.0019 (5)	−0.0006 (5)	0.0031 (5)
C3	0.0479 (11)	0.0303 (9)	0.0548 (12)	0.0016 (8)	0.0029 (10)	0.0144 (9)

Geometric parameters (Å, º)

P1—O2	1.4916 (11)	N1—C1	1.484 (2)
P1—O3	1.4924 (14)	N1—C2^{ii}	1.5020 (19)
P1—O1	1.5389 (15)	C1—C2	1.514 (2)
P1—O4	1.5884 (8)	C2—N1^{ii}	1.5020 (19)
O4—P1^{i}	1.5884 (8)	C2—C3	1.510 (2)

O2—P1—O3	116.60 (8)	P1—O4—P1^{i}	135.50 (12)
O2—P1—O1	111.76 (8)	C1—N1—C2^{ii}	112.80 (12)
O3—P1—O1	108.96 (9)	N1—C1—C2	111.58 (12)
O2—P1—O4	107.67 (5)	N1^{ii}—C2—C3	109.69 (14)
O3—P1—O4	108.40 (8)	N1^{ii}—C2—C1	108.68 (11)
O1—P1—O4	102.44 (9)	C3—C2—C1	111.29 (15)

Symmetry codes: (i) −*x*+1, *y*, −*z*+1/2; (ii) −*x*+1, −*y*+1, −*z*+1.

Hydrogen-bond geometry (Å, º)

D—H···*A*	*D*—H	H···*A*	*D*···*A*	*D*—H···*A*
O1—H1···O3^{iii}	0.88 (3)	1.61 (3)	2.460 (2)	161 (3)
N1—H1*A*···O2^{iv}	0.90 (2)	1.86 (2)	2.7454 (17)	167 (2)
N1—H1*B*···O2	0.90 (2)	1.87 (2)	2.7543 (17)	168 (2)
C1—H1*C*···O3^{v}	0.982 (19)	2.353 (19)	3.193 (2)	143.0 (15)
C1—H1*D*···O1^{vi}	0.970 (19)	2.41 (2)	3.205 (2)	139.1 (15)
C2—H2···O3^{i}	1.00 (2)	2.53 (2)	3.344 (2)	138.3 (15)

Symmetry codes: (i) −*x*+1, *y*, −*z*+1/2; (iii) −*x*+3/2, *y*−1/2, −*z*+1/2; (iv) −*x*+3/2, −*y*+1/2, −*z*+1; (v) *x*, −*y*+1, *z*+1/2; (vi) −*x*+3/2, *y*+1/2, −*z*+1/2.